Plant Physiology, March 1999, Vol. 119, pp. 817–828, www.plantphysiol.org © 1999 American Society of Plant Physiologists

NADH-Glutamate Synthase in Alfalfa Root Nodules. Genetic Regulation and Cellular Expression[1]

Gian B. Trepp, Martijn van de Mortel, Hirofumi Yoshioka, Susan S. Miller, Deborah A. Samac, J. Stephen Gantt, and Carroll P. Vance*

Institut für Pflanzenwissenschaften Eidgenössische Technische Hochschule-Zürich, 8092 Zürich, Switzerland (G.B.T.); Department of Agronomy and Plant Genetics (G.B.T., M.v.d.M., H.Y., S.S.M., C.P.V.), Department of Plant Pathology (D.A.S.), and Department of Plant Biology (J.S.G.), University of Minnesota, 411 Borlaug Hall, 1991 Upper Buford Circle, St. Paul, Minnesota 55108; Plant Pathology Laboratory, Nagoya University, Chikusa, Nagoya 464–01, Japan (H.Y.); and United States Department of Agriculture, Agricultural Research Service, Plant Science Research Unit, 411 Borlaug Hall, 1991 Upper Buford Circle, University of Minnesota, St. Paul, Minnesota 55108 (D.A.S., C.P.V)

NADH-dependent glutamate synthase (NADH-GOGAT; EC 1.4.1.14) is a key enzyme in primary nitrogen assimilation in alfalfa (*Medicago sativa* L.) root nodules. Here we report that in alfalfa, a single gene, probably with multiple alleles, encodes for NADH-GOGAT. In situ hybridizations were performed to assess the location of NADH-GOGAT transcript in alfalfa root nodules. In wild-type cv Saranac nodules the *NADH-GOGAT* gene is predominantly expressed in infected cells. Nodules devoid of bacteroids (empty) induced by *Sinorhizobium meliloti* 7154 had no NADH-GOGAT transcript detectable by in situ hybridization, suggesting that the presence of the bacteroid may be important for NADH-GOGAT expression. The pattern of expression of NADH-GOGAT shifted during root nodule development. Until d 9 after planting, all infected cells appeared to express NADH-GOGAT. By d 19, a gradient of expression from high in the early symbiotic zone to low in the late symbiotic zone was observed. In 33-d-old nodules expression was seen in only a few cell layers in the early symbiotic zone. This pattern of expression was also observed for the *nifH* transcript but not for leghemoglobin. The promoter of *NADH-GOGAT* was evaluated in transgenic alfalfa plants carrying chimeric β-glucuronidase promoter fusions. The results suggest that there are at least four regulatory elements. The region responsible for expression in the infected cell zone contains an 88-bp direct repeat.

In most plants primary assimilation of inorganic N results from the collaborative activity of two enzymes, GS (EC 6.3.1.2) and GOGAT (EC 1.4.1.14) (Lea et al., 1990; Lam et al., 1996). GS catalyzes the ATP-dependent amination of glutamate, producing Gln. GOGAT catalyzes the reductive transfer of the amido group of Gln to the α-keto position of 2-oxoglutarate, yielding two molecules of glutamate (Boland and Benny, 1977). GOGAT, together with GS, maintains the flow of N from NH_4^+ into Gln and glutamate. These products are then used for several other aminotransferase reactions in the synthesis of amino acids (Lea et al., 1990). Kinetic and inhibitory studies suggest that GOGAT is the rate-limiting step through the GS/GOGAT cycle (Chen and Cullimore, 1989; Baron et al., 1994).

In higher plants GOGAT occurs as two distinct forms, using Fd or NADH as a reductant. In addition to reductant specificity, the enzymes differ in molecular mass, kinetics, and antigenicity (Lea et al., 1990; Temple et al., 1998). Fd-GOGAT (EC 1.4.7.1) is localized in chloroplasts (Wallsgrove et al., 1979; Becker et al., 1993). The monomeric enzyme is suggested to be an Fe-S protein (Hirasawa and Tamura, 1984; Knauff et al., 1991) with a molecular mass of 140 to 160 kD (Lea et al., 1990; Temple et al., 1998). Fd-GOGAT cDNAs have been cloned from maize (Sakakibara et al., 1991), tobacco (Zehnacker et al., 1992), barley (Avila et al., 1993), alfalfa (Vance et al., 1995), Arabidopsis (Lam et al., 1996), and spinach (Nalbantoglu et al., 1994). Application of NO_3^-, which strongly induces nitrate reductase (EC 1.6.6.1), has only a minor effect on the expression of Fd-GOGAT in leaves, suggesting that the major role of Fd-GOGAT is probably the reassimilation of ammonia derived through photorespiration (Somerville and Ogren, 1980; Kendall et al., 1986; Sakakibara et al., 1992).

Like Fd-GOGAT, the plant NADH-GOGAT protein (EC 1.4.1.14) is a monomer with a molecular mass of 200 to 240 kD (Gregerson et al., 1993b; Vance et al., 1995; Temple et al., 1998). cDNA clones have been reported for Arabidopsis (Lam et al., 1996) and alfalfa (Gregerson et al., 1993b), and the enzyme has been purified from pea (Chen and Cullimore, 1988), lupine (Boland and Benny, 1977), rice (Hayakawa et al., 1992), and alfalfa (Anderson et al., 1989). Additionally, genes corresponding to a rice (Goto et al., 1998) and an alfalfa NADH-GOGAT cDNA (Vance et al., 1995) have been isolated and characterized. In alfalfa the NADH-GOGAT transcript is 7.2 kb long and encodes a 2194-amino acid protein, including a 101-amino acid precursor peptide. The *NADH-GOGAT* gene is 14 kb long and

[1] This work was supported in part by National Science Foundation grant no. IBN-9206890 and ETH-Zurich fellowship no. 0-28-001-91. This paper is a joint contribution from the Plant Science Research Unit, U.S. Department of Agriculture, Agricultural Research Service, and the Minnesota Agricultural Experiment Station (paper no. 98-1-13-0100, Scientific Journal Series).

*Corresponding author; e-mail vance004@maroon.tc.umn.edu; fax 1–651–649–5058.

Abbreviations: GOGAT, Glu synthase; GS, Gln synthetase.

is composed of 22 exons interrupted by 21 introns. In green tissues of alfalfa NADH-GOGAT enzyme activity and the abundance of its mRNA is low to nondetectable (Gregerson et al., 1993b). However, NADH-GOGAT activity increases severalfold during alfalfa root nodule development (Gregerson et al., 1993b) and is the major form of GOGAT in this tissue (Vance et al., 1995). This increase corresponds with an increase in enzyme protein and mRNA (Gregerson et al., 1993b). Moreover, this increase in NADH-GOGAT expression appears to be restricted to nodules capable of N_2 fixation. In contrast, other nodule-enhanced enzymes involved in N_2 assimilation, such as aspartate aminotransferase (EC 2.6.1.1), GS, PEP carboxylase (EC 4.1.1.31), and Asn synthetase (EC 6.3.5.4), were expressed in both effective and ineffective nodules (Groat and Vance, 1981; Vance and Gantt, 1992; Vance et al., 1994).

Further understanding of the regulation of *NADH-GOGAT* in alfalfa nodules necessitates the identification of cellular patterns of transcript accumulation and the definition of elements in the 5′ flanking region of the gene that controls expression in nodules. In this report we document NADH-GOGAT transcript accumulation in cells of both effective and ineffective nodules during root nodule development and relate this expression to that of nitrogenase and leghemoglobin. In addition, promoter deletion analysis using the GUS reporter gene in transgenic alfalfa is performed to define elements controlling root nodule specificity.

MATERIALS AND METHODS

Plant Material and Bacterial Strains

Alfalfa (*Medicago sativa* L.) cv Saranac and a single gene-recessive genotype "ineffective Saranac" (in_1 Saranac) forming non-N_2-fixing, early-senescing nodules (Peterson and Barnes, 1981) were used in this study. Seeds were obtained from Dr. J.F.S. Lamb (U.S. Department of Agriculture, Agricultural Research Service, St. Paul, MN). Although alfalfa is an outcrossing-tetraploid species, precluding the formation of isogenic lines, more than 90% of the in_1 Saranac genotype comes from the cv Saranac background.

Plants of these two genotypes were maintained in greenhouse sand benches and inoculated with effective *Sinorhizobium meliloti* 102F51 as described by Egli et al. (1989). For analysis of NADH-GOGAT expression in bacterial conditioned ineffective nodules, cv Saranac seeds were surface-sterilized (70% ethanol for 10 min) and planted in sterilized sand inoculated with ineffective *S. meliloti* F642, *dctA* (dicarboxylic acid uptake deficient; Yarosh et al., 1989) or 7154, *exoH* (acid exopolysaccharide succinylation deficient; Leigh et al., 1987). These strains were generous gifts of Turlough Finan (McMaster University, Hamilton, Ontario, Canada) and Ann Hirsch (University of California, Los Angeles), respectively. The plants inoculated with mutant *Sinorhizobium* strains were grown in growth chambers (Conviron PGV 36, Controlled Environment, Ltd., Winnipeg, Manitoba, Canada[2]). To exclude contamination with wild-type *Sinorhizobium*, nitrogenase activity was assayed as H_2 evolution in an open-flow system adapted from Minchin et al. (1983) using a nitrogenase-activity analysis system (Morgan Scientific, Haverhill, MA). For all studies the planting date was designated as d 0.

PCR for NADH-GOGAT

Two degenerate oligonucleotide primers were synthesized for the amplification of NADH-GOGAT genomic sequences. Each primer is complementary to conserved sequences in the Fd-GOGAT of tobacco (Zehnacker et al., 1992) and barley (Avila et al., 1993) and the NADH-GOGAT of alfalfa (Gregerson et al., 1993b) and *Escherichia coli* (Oliver et al., 1987) (see Fig. 1). The primer sequences are as follows: primer 1, GCNAT(A/C/T)AA(A/G)CA (A/G)GTNC; primer 2, CCNCCNGTCAT(A/G)TA(T/C) TC(A/G)CA. Fifty microliters of PCR reaction contained 0.1 μg of genomic alfalfa DNA, 2.5 mM $MgCl_2$, 1× *Taq* DNA polymerase buffer (50 mM KCl, 10 mM Tris-HCl, 0.1% Triton X-100, pH 9.0) (Promega), 200 μM of each deoxyribonucleotide triphosphate, 25 pmol of primer, and 5 units of *Taq* DNA polymerase (Promega). PCR was performed for 30 cycles and the amplification conditions were 95°C for 1 min followed by 45°C for 30 s and 72°C for 2 min; final elongation was at 72°C for 5 min. The amplification products were purified and cloned into a pGEM-T vector (Pharmacia). The PCR product was sequenced by chain terminators with the T7 primer using Sequenase (Amersham). Sequence analysis was performed using the Genetics Computer Group (Madison, WI) sequence-analysis software package.

Preparation of RNA Probes

All probes used in this study were generated from linearized pBluescript KS^+ plasmids (Stratagene), containing a 1.8-bp (*Bam*HI-*Not*I) NADH-GOGAT cDNA fragment (Gregerson et al., 1993b), a 1.1-bp *nifH* gene fragment, or a 0.9-bp leghemoglobin cDNA fragment. Each construct was linearized with the appropriate enzymes and transcribed in the sense and antisense directions using T3 or T7 RNA polymerases and [^{35}S]UTP as described by the manufacturer (Stratagene). The *nifH* gene fragment and the leghemoglobin cDNA fragment were generous gifts from Mike Sadowsky (University of Minnesota, St. Paul) and Ann Hirsch, respectively. The probes were partially degraded to a length of 150 nucleotides by heating at 60°C in a 0.06 M Na_2CO_3/0.04 M $NaHCO_3$ solution (Cox and Goldberg, 1988).

In Situ Hybridization

The tissue for all in situ hybridizations was collected as follows. The planting date is considered to be d 0; at

[2] Mention of a trademark, proprietary product, or vendor does not constitute a guarantee or warranty of the product by the U.S. Department of Agriculture and does not imply its approval to the exclusion of other products or vendors that might also be suitable.

harvest dates, only the two top root nodules on the main root were used for subsequent studies. In situ hybridization was carried out essentially as described by Fleming et al. (1993). Tissues were fixed in 4% paraformaldehyde and 0.25% glutaraldehyde in 50 mM sodium phosphate buffer, pH 7.2. The tissues were then rinsed twice in the same buffer and twice in deionized water, and dehydrated in a graded ethanol series. After the absolute ethanol was replaced with xylene, tissues were embedded in Paraplast (Oxford Labware, St. Louis, MO). The embedded tissues were sectioned at a thickness of 7 μm and affixed to poly-L-Lys-coated slides. Hybridizations were performed in mineral oil as described by Heintzen et al. (1994), and the final wash conditions were 0.1× SSC (1× SSC = 0.15 M NaCl, 15 mM sodium citrate) including 1 mM DTT at 50°C for 20 min. In situ hybridization slides of effective nodules were exposed to emulsion for 10 to 14 d, and those performed with ineffective nodules were exposed for 26 to 28 d. After development the sections were stained with 0.05% toluidine blue O, dehydrated, and mounted with Permount (Fisher Scientific). Sections were viewed and photographed with a Labophot microscope (Nikon) equipped with dark- and bright-field optics.

Construction of Chimeric Genes and Plant Transformation

Standard DNA techniques were used for DNA manipulations (Sambrook et al., 1989). Sequence analyses of these chimeric genes demonstrated that each insert was correctly cloned. Nine promoter constructs were generated, one transcriptional and eight translational fusions. The 3′ end of the transcriptional fusion (GScript) is 103 bp 5′ of the translational start codon of *NADH-GOGAT*. Constructs GLate and G1 through G7 are translational fusions to the GUS gene, and the 3′ end of all these constructs is 8 bp past the ATG of the *NADH-GOGAT* gene. GLate, G5, and G7 are restriction fragments from the originally isolated 5′ upstream region of the *NADH-GOGAT* gene. G1, G2, G3, G4, and G6 are PCR products that have been amplified using a common 3′ primer and a specific 5′ primer. All promoter sequences were cloned in the vector pBI101.2 (Clontech, Palo Alto, CA).

The promoter-GUS constructions were introduced into *Agrobacterium tumefaciens* LB4404 by electroporation. Transgenic alfalfa plants were obtained essentially as described by Austin et al. (1995) using a clone selected from the alfalfa cultivar, RegenSY (Bingham, 1991). Regenerated plants were propagated by cuttings. Verification that plants were transformed with the respective constructs was obtained by PCR analysis of DNA extracted from the regenerated plants. Cuttings were maintained in vermiculite and inoculated with *S. meliloti* strain 102F51. Nodule tissues were collected 12 to 26 d after inoculation for GUS enzymatic assays and histochemical detection.

Analysis of GUS Activity

The detection of GUS activity in nodules was performed by the procedure described by Jefferson (1987). The GUS-stained tissues were fixed in 4% paraformaldehyde and 0.25% glutaraldehyde in 50 mM sodium phosphate buffer, pH 7.2, rinsed in deionized water, and stored in 70% ethanol until they were photographed. GUS activity was determined as described by Jefferson (1987). Nodules were collected and homogenized in extraction buffer. After centrifugation the supernatant was used to quantitate GUS activity using 4-methylumbelliferyl β-D-glucuronic acid as a substrate. Tissues from regenerated nontransformed plants were used to quantitate background activity. Enzyme activity was determined with a minifluorometer (TKO-100; Hoefer Scientific, San Francisco, CA). The protein concentration was determined using protein assay (Bio-Rad). The kinetic data obtained were further analyzed using a statistical program (Statistix, Analytical Software, Tallahassee, FL). Because the sample population for each promoter-deletion construct did not have a normal distribution, the data were transformed ($\log[x + 1]$) to achieve homogeneity of variance. The transformed data were then analyzed using analysis of variance and the corresponding LSD was calculated. The level of significance was set at $P < 0.01$. Because many differences in GUS activity for adjacent promoter constructs were not significant, we further analyzed the data using linear regression. Therefore, the transformed means were plotted against the corresponding length of the deletion (bp) ($1/\log[\text{bp} + 1]$). We found a positive linear relation between deletion length and GUS activity (r^2 adjusted = 73.37%; $P = 0.0041$).

RESULTS

Screening for Other NADH-GOGAT Isoforms in the Alfalfa Genome by PCR

To determine if there are other NADH-GOGAT isoforms in alfalfa, we designed degenerate primers from the conserved regions of the deduced amino acid sequence of Fd-GOGAT from tobacco (Zehnacker et al., 1992) and barley (Avila et al., 1993) and the NADH-GOGAT from alfalfa (Gregerson et al., 1993b) and *E. coli* (Oliver et al., 1987) (Fig. 1). PCR reactions were performed with alfalfa genomic DNA (cv Saranac), and all PCR products of at least the size of the corresponding NADH-GOGAT cDNA fragment (1.4 bp) were cloned into pGEM-T (Pharmacia). Fourteen positive clones derived from four independent PCR reactions were greater than 99% similar to the originally reported

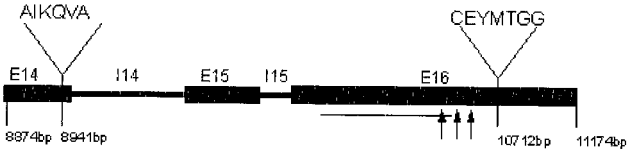

Figure 1. Diagrammatic representation of the portion of the alfalfa *NADH-GOGAT* gene used for PCR. Exons are indicated by boxed regions, and introns are represented by lines. PCR was performed over three exons (exon 14 [E14], exon 15 [E15], exon 16 [E16]) and two introns (intron 14 [I14] and intron 15 [I15]) of the reported alfalfa gene using primer 1 (AIKQVA) and primer 2 (CEYMTGG). The putative binding for the (Fe-S) cluster is indicated by arrows, and the putative flavin mononucleotide binding site is underlined.

NADH-GOGAT gene (Vance et al., 1995) for exon as well as intron sequences.

Localization of NADH-GOGAT mRNA in Alfalfa Root Nodules by in Situ Hybridization

To localize the NADH-GOGAT transcript in root nodules, we performed in situ hybridization. Nodule ultrastructure was classified based on the nomenclature of Vasse et al. (1990). Five distinct zones were defined along the axis in a longitudinal section through an alfalfa nodule: the nodule meristem (zone I), passing to the invasion zone (zone II), the amyloplast-rich interzone (zones II–III [*]), the N_2-fixing zone and proximal inefficient zone (zone III), and the senescent zone (zone IV) (Figs. 2A and 3G). When sections of a 19-d-old nodule were hybridized with a NADH-GOGAT antisense RNA probe, hybridization specific for NADH-GOGAT mRNA, seen in the dark field as a bright silver grain, was observed in the interzone and the N_2-fixing zone (Fig. 2, A and B). No NADH-GOGAT transcript was detected in the meristem (Fig. 2, C and F), the invasion zone (Fig. 2, C and D), or the cortical tissue (Fig. 2, E and F). Enhanced *NADH-GOGAT* gene expression began just adjacent to the invasion zone (Fig. 2, C and D). Little NADH-GOGAT hybridization signal was found in uninfected cells (Fig. 2, C–H), suggesting that NADH-GOGAT is predominantly expressed in the infected cells. No significant hybridization signal was obtained when alfalfa root nodules were probed with a NADH-GOGAT sense RNA probe (Fig. 2, I–L).

In Situ Localization of NADH-GOGAT mRNA during the Development of Effective and Ineffective Nodules

We previously reported an increase in the abundance of NADH-GOGAT-specific transcripts in RNA isolated from developing effective nodules, from d 8 after inoculation to d 33. A comparable increase was not detected in either plant- or bacteria-controlled ineffective nodules (Gregerson et al., 1993b; Vance et al., 1994). To study the regulation of the *NADH-GOGAT* gene during nodule development in effective cv Saranac and plant-controlled ineffective cv Saranac nodules, in situ hybridizations were performed comparing the spatial and temporal expression patterns of NADH-GOGAT using 7-, 9-, 19-, and 33-d-old nodules. Hybridization specific for NADH-GOGAT mRNA was detected in effective 7-d-old nodules 2 d before the onset of N_2 fixation (Fig. 3, A and B) (Gantt et al., 1992; G.B. Trepp and C.P. Vance, unpublished results). Similarly, ineffective nodules also had a detectable hybridization signal for the NADH-GOGAT transcript at this time (Fig. 3, I and J). By d 9, at the onset of N_2 fixation (Gantt et al., 1992; G.S. Trepp and C.P. Vance, unpublished results), we observed a strong signal in the infected cells of effective nodules throughout the central nodule tissue (Fig. 3, C and D). In plant-controlled ineffective nodules hybridization to NADH-GOGAT mRNA was also observed in the infected cells (Fig. 3, K– N). As a result of early senescence the nodules generally contained a smaller number of infected cells (Fig. 3, M and N). In these ineffective nodules the signal representing NADH-GOGAT transcript was observed in a thin layer of cells behind the invasion zone where the infected cells were intact.

At d 19 effective nodules had a very strong signal for NADH-GOGAT transcript in the infected cells. Expression was highest in the interzone and decreased gradually to a low signal in the proximal regions of the nodule (Fig. 3, E and F). In contrast, every 19-d-old ineffective cv Saranac nodule examined contained large senescing zones. Additionally, the infected cells in these nodules were arranged in two patterns. One formed an enlarged 8- to 15-cell-wide symbiotic zone followed by a large senescent zone (Fig. 3, O and P), and the second formed a very short 2- to 4-cell-wide symbiotic zone followed by a large senescent zone (Fig. 3, Q and R). In both types the signal appeared to be restricted to the infected cells. In 33-d-old nodules the in situ hybridization signal for NADH-GOGAT mRNA in cv Saranac nodules was observed only in the 5- to 15-cell-wide zone including the interzone and the distal part of the N_2-fixing zone (Fig. 3, G and H). No NADH-GOGAT transcripts were apparent in the proximal part of the N_2-fixing zone or the senescent zone. The signal specific for NADH-GOGAT mRNA at 33 d in ineffective nodules had the same distribution pattern that was described for the effective nodule (Fig. 3, S and T). However, hybridization was very weak and several attempts had to be made to obtain a sufficient signal.

Localization of NADH-GOGAT, *nifH*, and Leghemoglobin in 33-d-old Alfalfa Root Nodules Using Serial Sections

We performed in situ hybridizations to test whether the expression pattern of *NADH-GOGAT* in 33-d-old nodules was unique or whether this is a common pattern for genes involved in N_2 fixation. We made serial sections, which allowed us to directly compare the expression patterns of *NADH-GOGAT*, a subunit of the nitrogenase protein (*nifH*), and leghemoglobin (*mslbc3*) in the same nodule. The signal for NADH-GOGAT mRNA agrees with the previously described pattern (Fig. 3, G and H). *NADH-GOGAT* gene expression was detected in a 5- to 15-cell-wide zone including the interzone (zone II–III [*]) and the N_2-fixing zone (zone III) (Fig. 4, A and B). The signal corresponding to leghemoglobin gene expression was detected throughout the nodule interior, including the invasion zone (zone II), the interzone (zone II–III [*]), and the N_2-fixing zone (zone III). However, expression appeared strongest in a 5- to 15-cell-wide zone including the interzone (zone II–III [*]) and the N_2-fixing zone (zone III) (Fig. 4, C and D). The signal specific for *nifH* gene expression was in the N_2-fixing zone (zone III) in a 5- to 15-cell-wide area similar to that observed for NADH-GOGAT (Fig. 4, E and F).

Localization of NADH-GOGAT Transcripts in Ineffective Nodules Formed on Effective cv Saranac by Ineffective *S. meliloti* Strains

NADH-GOGAT appears to be expressed predominantly in infected cells. We addressed the question of whether the

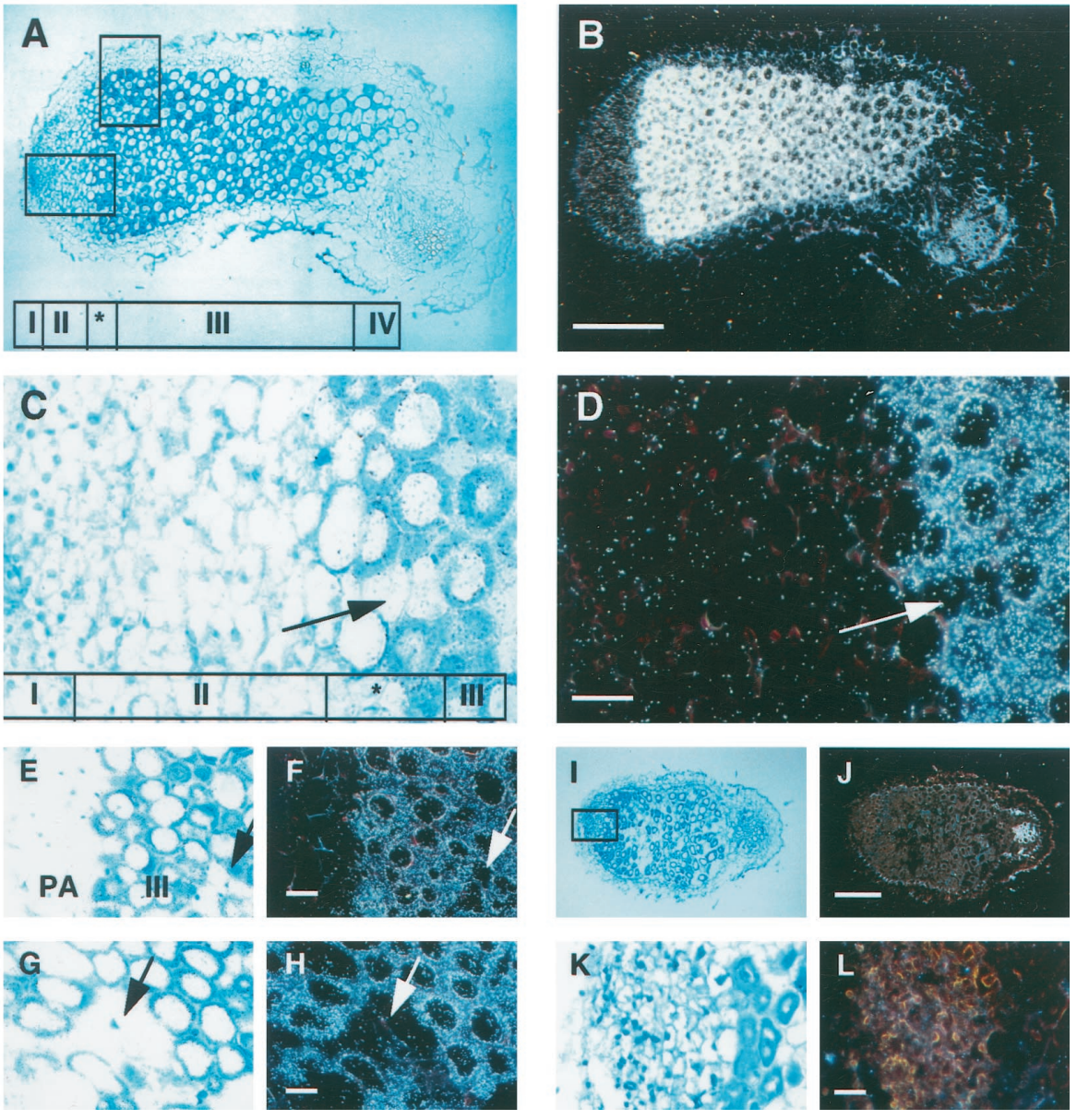

Figure 2. Localization of NADH-GOGAT mRNA in alfalfa root nodules by in situ hybridization. Bright-field (A, C, E, G, I, and K) and dark-field (B, D, F, H, J, and L) photographs of a longitudinal section through 19-d-old effective alfalfa nodules. Nodule ultrastructure was classified based on the nomenclature of Vasse et al. (1990): meristem (zone I), invasion zone (zone II), interzone (*), N_2-fixing zone (zone III), and senescent zone (zone IV). The nodule in A to H was hybridized with NADH-GOGAT ^{35}S-labeled antisense RNA probe. Enlargement of the lower boxed region in A shown in bright-field (C) and dark-field (D) photographs includes a portion of the meristem (zone I), invasion zone (zone II), and interzone (*). Enlargement of the upper box in A shown in bright-field (E) and dark-field (F) photographs includes the central zone (III), including parenchymal tissue (PA). In bright-field (G) and dark-field (H) photographs of infected and uninfected cells, arrows in C through H point to uninfected cells. Bright-field (I and K) and dark-field (J and L) photographs of a longitudinal section through a 19-d-old effective alfalfa nodule hybridized with NADH-GOGAT ^{35}S-labeled sense RNA probe. Bars in B and J = 800 μm; bars in D, F, H, and L = 80 μm.

presence of *S. meliloti* was necessary for *NADH-GOGAT* gene expression in root nodules. Therefore, we examined ineffective nodules derived through the infection of two *S. meliloti* fix$^-$ mutants.

Nodules formed by *S. meliloti* F642, which is deficient in dicarboxylic acid transport (Yarosh et al., 1989), are generally much smaller than wild-type nodules. These nodules contain *S. meliloti*; however, the *S. meliloti* does not differentiate into fully developed bacteroids and therefore cannot fix atmospheric dinitrogen. In 19-d-old nodules induced by *S. meliloti* F642, NADH-GOGAT transcripts were detected in the infected cells (Fig. 5, A and B). The transcript abundance is low, comparable to that of ineffective cv Saranac.

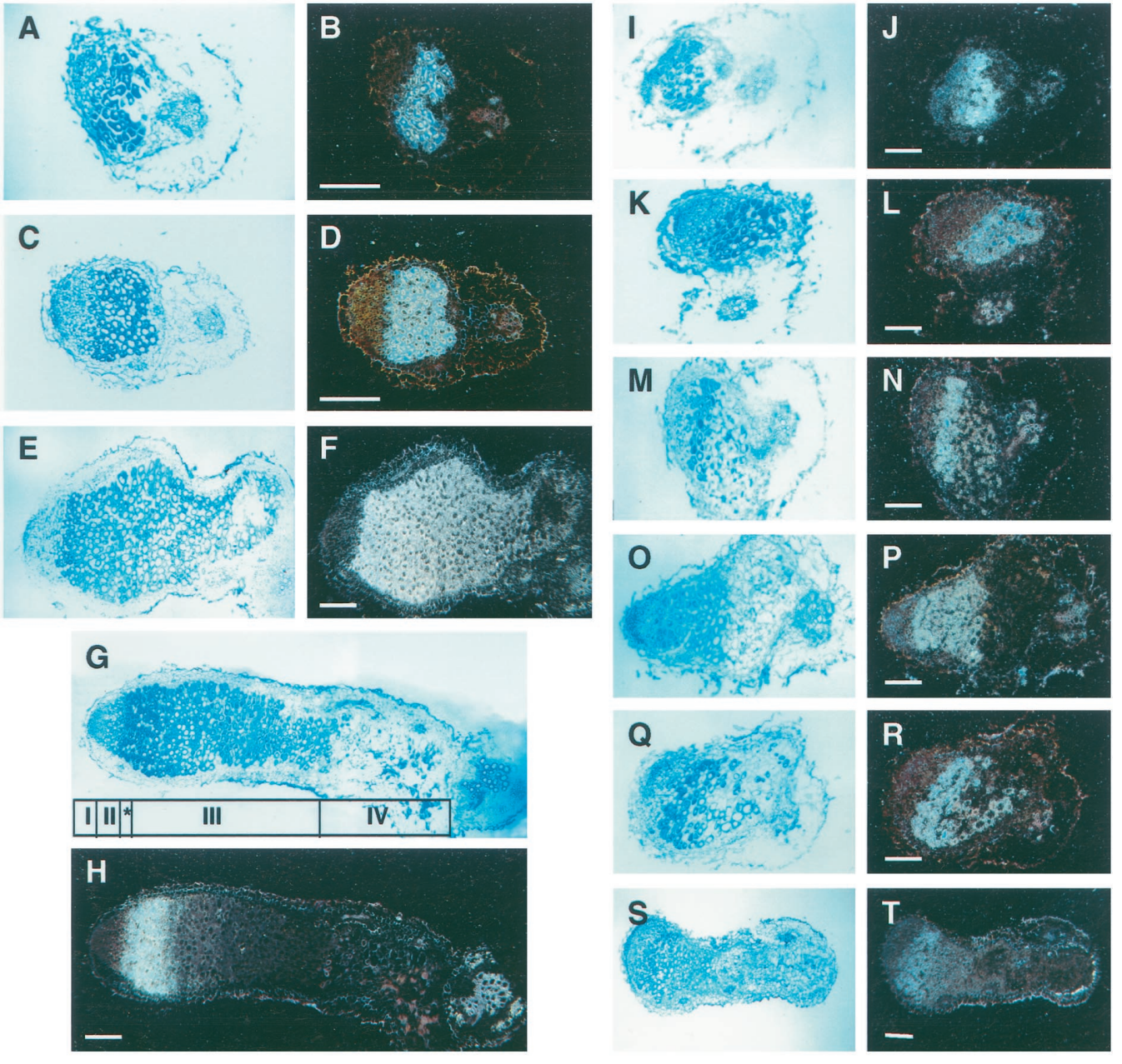

Figure 3. Localization of NADH-GOGAT transcript in effective and plant-gene-controlled ineffective alfalfa nodules during development. Longitudinal sections through effective (A–H) and plant-controlled ineffective (I–T) alfalfa root nodules. The bright-field and dark-field image pairs are of 7- (A, B, I, and J), 9- (C, D, K, L, M, and N), 19- (E, F, O, P, Q, and R), and 33- (G, H, S, and T) d-old root nodules. Bars = 400 μm.

S. meliloti strain 7154 (Leigh et al., 1987), which is deficient in the acid exopolysaccharide succinylation, induces aborted infection threads and thus the *S. meliloti* is not released into plant cells. *S. meliloti* 7154 is able to induce the formation of root nodules; however, they are tumor-like, non-N_2-fixing nodules. In 19-d-old nodules formed by *S. meliloti* 7154, we were unable to detect a significant hybridization signal to NADH-GOGAT transcripts (Fig. 5, D and E). Control experiments performed with sense riboprobes showed no significant hybridization signal (Fig. 5, C and F).

Analysis of the 5′ Upstream Region of the *NADH-GOGAT* Gene in Transgenic Alfalfa Plants

Our previous data (Gregerson et al., 1993b; Vance et al., 1995) demonstrated that during the development of effective alfalfa nodules NADH-GOGAT transcripts increased some 10- to 20-fold, whereas roots and leaves accumulated little or no transcript. Moreover, a translational fusion made with the putative promoter region of NADH-GOGAT fused to the GUS gene directed reporter gene activity to the nodules of alfalfa and trefoil (Vance et al.,

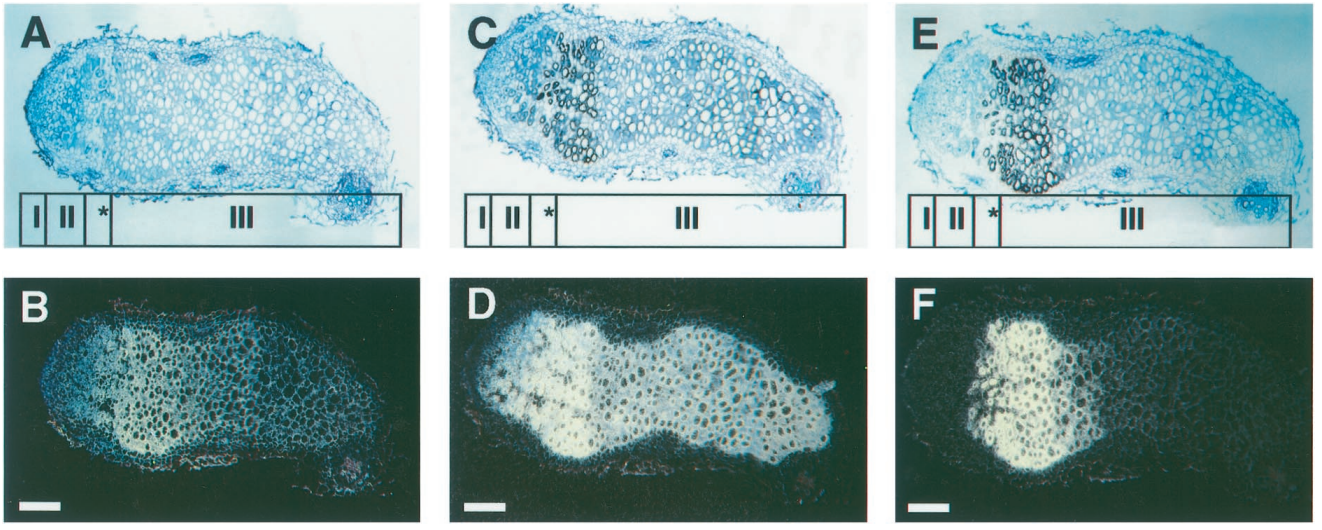

Figure 4. In situ localization of the NADH-GOGAT, *nifH*, and leghemoglobin transcripts in 33-d-old alfalfa root nodules using serial sections. The bright-field and dark-field image pairs are of longitudinal sections through 33-d-old root nodules that were hybridized with ^{35}S-labeled NADH-GOGAT (A and B), leghemoglobin (C and D), or *nifH* (E and F) antisense RNA probe. Bars = 400 μm.

1995). These data, together with the in situ hybridization results described above, led us to further investigate the transcriptional regulation of the *NADH-GOGAT* gene. To further investigate that the 5′ flanking region of *NADH-GOGAT* conferred expression in root nodules, GUS enzyme activity was evaluated in alfalfa plants transformed with either a translational (GLate) or a transcriptional (GScript) fusion. GUS enzyme activity was 3- to 20-fold higher in nodules than in leaves, stems, and roots, irrespective of whether reporter gene activity was controlled by a translational (GLate) or a transcriptional (GScript) *NADH-GOGAT* promoter construct (Table I). The differences in

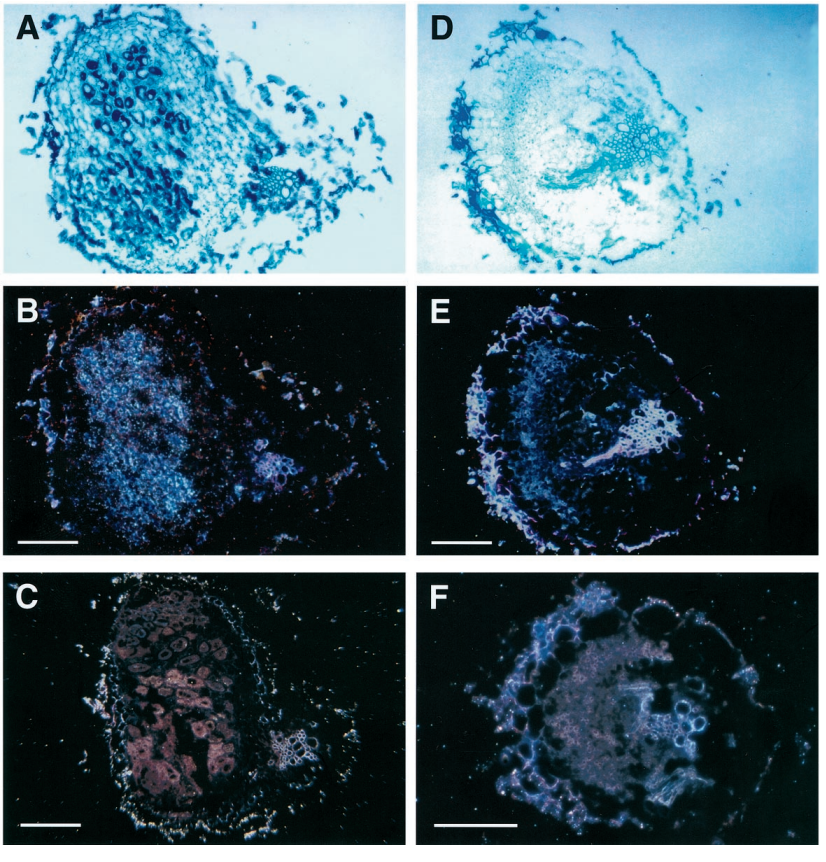

Figure 5. In situ localization of NADH-GOGAT transcripts in nodules induced by *S. meliloti* F642 and 7154. The bright-field (A and D) and dark-field (B, C, E, and F) images are of longitudinal sections through 19-d-old root nodules induced by *S. meliloti* F642 (A–C) and *S. meliloti* 7154 (D–F). The sections in A, B, D, and E were hybridized with ^{35}S-labeled NADH-GOGAT antisense RNA probe, whereas those in C and F were hybridized with sense riboprobes and photographed under dark-field conditions. Bars = 400 μm.

Table I. *Organ-specific GUS activity ±SE in transgenic alfalfa containing the GUS gene driven by the NADH-GOGAT promoter*

Construct	Plants	Mean GUS Activity			
		Leaf	Stem	Root	Nodule
	no.	*pmol min^{-1} mg^{-1} protein*			
GLate[a]	16[b]	132 ± 132	461 ± 204	338 ± 134	1,205 ± 1,837
GScript[a]	21[b]	140 ± 123	257 ± 190	266 ± 131	2,006 ± 1,197
35S GUS[d]	NA[c]	17,900	22,800	5,700	5,000

[a] GLate, Translational fusion; GScript, transcriptional fusion; 2.7 bp of the 5′ upstream region of the *NADH-GOGAT* gene fused to the GUS reporter gene. [b] No. of independent transformants evaluated. [c] NA, Not applicable. [d] Transgenic alfalfa containing the GUS reporter gene driven by the cauliflower mosaic virus 35S promoter.

GUS enzyme activity between GLate and GScript were not significant. In an attempt to identify elements in the 5′ flanking region of the gene that direct and limit expression to the root nodule, chimeric reporter genes were constructed containing sequences of various lengths upstream of the transcriptional start site fused to GUS (Fig. 6). These constructs were used to transform alfalfa, and the regenerated plants were assayed for GUS activity and stained for histochemical localization of GUS (Fig. 6A). GUS activity in transgenic plants was quantified by a fluorometric assay (Jefferson, 1987) (Fig. 6B). Nodules taken from plants containing the longest deletion, GLate (−2700), had the greatest total GUS activity. Although total GUS activity was reduced in nodules from plants containing deletions G1, G2, G3, and G4, statistical analysis of adjacent deletions showed no significant differences ($P < 0.01$). However, when the region between G4 (−356) and G5 (−241) was deleted, GUS activity decreased significantly ($P < 0.01$). In contrast, when the region from G5 (−241) to G6 (−151) was deleted, the GUS activity increased dramatically; the deletion of G6 (−151) to G7 (−82) reduced all GUS activity from nodules to background levels ($P < 0.01$).

The two largest constructs, GLate (−2700) and G1 (−1064), directed reporter gene activity to the N_2-fixing zone (zone III) of effective root nodules (Fig. 7, A and B), consistent with in situ hybridization data. However, it was not unusual to find the root nodule meristem (zone I), the invasion zone (zone II), and/or the vascular tissue staining in some plants carrying GLate and G1 promoter constructs. When the G1 construct was shortened, resulting in construct G2, significantly different patterns of GUS localization were noted (Fig. 7C). In root nodules the G2 promoter fragment (−655) directed reporter gene expression to the vascular tissue and/or the root nodule meristem, but not the central zone of the nodule. These data indicate that elements within the 5′ upstream region between G1 (−1064) and G2 (−655) control reporter-gene expression in the N_2-fixing zone. Within this region is an 88-bp direct repeat. Plants carrying deletions G3, G4, G5, and G6 had a staining pattern similar to that of plants carrying deletion G2 (data not shown). Construct G7 resulted in a loss of all GUS staining in nodules (Fig. 7D). These data indicate that two regions of the 5′ upstream region contribute to nodule activity. The region from −1064 to −655 appears to control

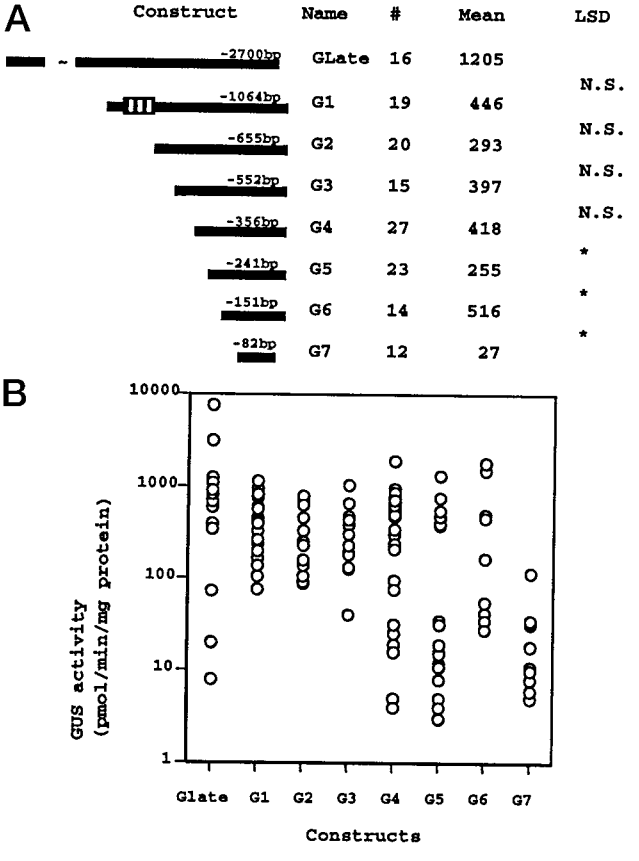

Figure 6. Diagram of the *NADH-GOGAT* promoter-GUS gene constructs. A, Eight sequences containing the putative *NADH-GOGAT* promoter were translational fusions to the GUS gene; the length of these truncations is measured with respect to the transcriptional start. The boxed region in construct G1 marks the location of the 88-bp direct repeat. The number of individual transformants tested for each construct is indicated (#). Mean GUS activity (pmol min^{-1} mg^{-1} protein) is indicated with the heading "Mean." LSD values between adjacent deletions were calculated, and the level of significance was set at $P < 0.01$. N.S., Not significant; *, significant at $P < 0.01$. B, Distribution of GUS activity per construct measured from individual independently transformed plants.

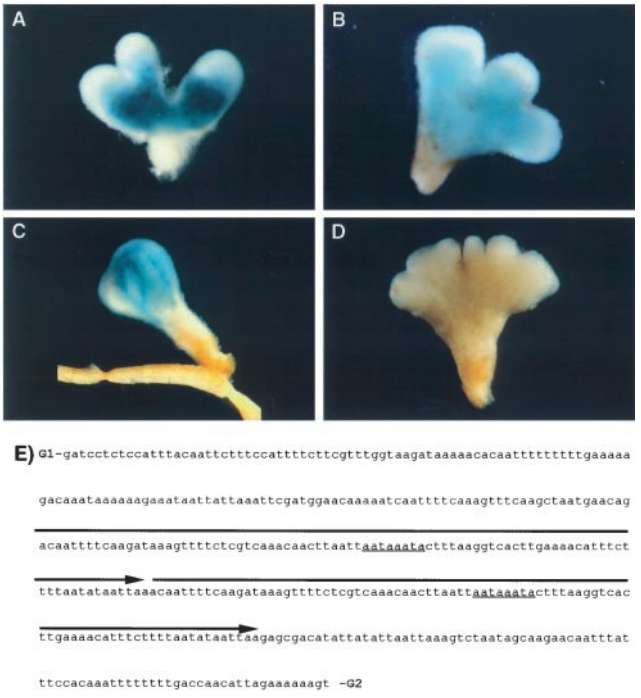

Figure 7. GUS staining of the *NADH-GOGAT* promoter deletions. For deletions GLate (A) and G1 (B), individual transformants with GUS activity close to the mean had a GUS staining pattern similar to the results obtained for in situ hybridizations. A loss in tissue specificity was observed in deletion G2 (C), whereas no GUS staining was observed in deletion G7 (D). E, The 409-bp region between deletion G1 and G2. The 88-bp direct repeat is overlined, and the location of the conserved octanucleotide motif is underlined.

reporter gene activity in the interior N_2-fixing zone, whereas the region from −155 to −89 contains elements that affect activity in other zones of the nodule.

DISCUSSION

To accurately determine the expression pattern of *NADH-GOGAT* in root nodules through in situ hybridization experiments and promoter deletion analysis studies, we thought it necessary to assess whether alfalfa contains multiple *NADH-GOGAT* genes. Previous results (Gregerson et al., 1993b; Vance et al., 1995) indicated that *NADH-GOGAT* occurred as either a small gene family or a single gene with multiple alleles. The fact that all PCR products amplified from genomic DNA with degenerate primers were greater than 99% identical across introns gives strong support for the latter interpretation. Additionally, the *NADH-GOGAT* gene has been mapped to a single locus on the genetic map of alfalfa (G.B. Kiss, personal communication). However, multiple alleles of a single gene would be expected in this outcrossing, tetraploid species. Multiple alleles have also been reported for the aspartate aminotransferase and PEP carboxylase genes (Gregerson et al., 1993a; Pathirana et al., 1997). A single form of *NADH-GOGAT* is also consistent with biochemical data showing a single form of NADH-GOGAT in alfalfa (Anderson et al., 1989). In contrast, two isoforms of NADH-GOGAT have been documented in bean root nodules (Chen and Cullimore, 1988), and a preliminary report suggests two distinct cDNAs (M. Lara, L. Blanco, and C.P. Vance, unpublished results).

In situ hybridization experiments give new insights into the regulation of the *NADH-GOGAT* gene in developing effective and ineffective alfalfa root nodules. The transcript specific for NADH-GOGAT is triggered in the infected cells of the interzone of alfalfa root nodules. Toward the proximal end of zone III (the N_2-fixing zone), *NADH-GOGAT* expression declines as infected cells become older. Similar results have been reported for leghemoglobin (de Billy et al., 1991), GS (Temple et al., 1995), and PEP carboxylase (Pathirana et al., 1997). The interzone seems to be an area where several developmental changes occur. In addition to the enhanced expression of several genes encoding enzymes of the N and C metabolism, bacteroid morphology shifts from nonfixing type 3 to larger, more pleiomorphic N_2-fixing type 4 (Vasse et al., 1990). Also in this region, plant cells enlarge substantially, amyloplasts accumulate, and in pea and vetch the expression of the early nodulins PsENOD5, PsENOD12, and VsENOD12 declines (Scheres et al., 1990; Franssen et al., 1992; Vijn et al., 1995).

In previous studies, which relied on RNA-blot analysis, we detected little to no NADH-GOGAT transcript in plant-controlled ineffective nodules (Gregerson et al., 1993b; Vance et al., 1995). The enhanced sensitivity of detection by in situ hybridization coupled to cellular localization of transcript allowed us to determine that NADH-GOGAT is expressed in plant-controlled ineffective nodules at d 7, synchronous with expression occurring in effective nodules. By d 9 and 19 in ineffective nodules, *NADH-GOGAT* expression was limited to only a few layers of infected cells. At these same times in the effective symbiosis, NADH-GOGAT transcripts were detected throughout the nodule. Although it is difficult to estimate precise quantitative differences in the amount of transcripts using in situ hybridization, it appears that the amount of NADH-GOGAT transcript is substantially lower in the cells of the ineffective symbiosis than in the cells of the effective symbiosis. Thus, not only do ineffective nodules have a reduced number of cells expressing *NADH-GOGAT*, but they also have a lower total amount of transcript.

The reduced amount of *NADH-GOGAT* gene expression probably results from several factors. Nodules formed on ineffective cv Saranac plants and nodules formed by *S. meliloti* F642 show early senescence. Egli et al. (1989) and Pladys and Vance (1993) showed cellular deterioration and enhanced proteolysis in 9-d-old ineffective cv Saranac nodules, resulting in a substantial reduction of infected cells. Alternatively, the reduced amount of transcript could be attributable to either the lack of NH_4^+ (or product derived from NH_4^+) or the failure of *S. meliloti* to become fully differentiated into competent bacteroids. Vasse et al. (1990) noted that bacteroids in ineffective cv Saranac do not develop beyond the type 3 stage. Bacteroids in this stage in normal N_2-fixing nodules are smaller, have a less pleiomorphic shape, and do not fix N_2 compared with type 4 bacteroids.

The intense hybridization of NADH-GOGAT transcript seen in infected cells and the absence of a hybridization signal in other developmental zones and uninfected cells suggest that the presence of bacteria/bacteroid may be a prerequisite for NADH-GOGAT expression. This point is further supported by the absence of NADH-GOGAT transcript in empty nodules induced by *S. meliloti* 7154. Although the presence of bacteria/bacteroid appears to be a prerequisite to trigger *NADH-GOGAT* transcription, expression does not require active nitrogenase. Two lines of evidence support this thinking. First, we found that *NADH-GOGAT* transcripts can be detected in 7-d-old nodules, significantly earlier than nitrogenase activity can be measured (Gantt et al., 1992). Second, transcripts of *NADH-GOGAT* can be detected, albeit at reduced levels, formed in response to fix$^-$ bacteria such as *S. meliloti* F642 or from the plant-controlled ineffective genotype in_1 Saranac.

Although the presence of bacteria/bacteroid may be a prerequisite to trigger *NADH-GOGAT* gene expression, a different mechanism may be involved in the down-regulation of the gene. In 33-d-old nodules *NADH-GOGAT* transcripts are restricted to a 5- to 15-cell-wide zone, including the interzone and the proximal part of the N_2-fixing zone. Although bacteroids are present in the distal part of 33-d-old nodules, no signal for the *NADH-GOGAT* transcript could be detected. By comparing *NADH-GOGAT* to *nifH* and leghemoglobin expression, it appears that the *NADH-GOGAT* expression pattern is similar to that of *nifH*, but not to that of leghemoglobin. Therefore, similar or common factors may be involved in the regulation of *NADH-GOGAT* and *nifH*. Vasse et al. (1990) reported that in the proximal part of the N_2-fixing zone, the bacteroid morphology changes from type 4 to type 5. Moreover, they suggested that the type 5 bacteroid is inefficient in N_2 fixation. It would be tempting to suggest that N_2 fixation is restricted to the areas where both *nifH* and *NADH-GOGAT* are expressed. However, additional data are needed to link the changes in bacteroid morphology with the disappearance of *nifH* and *NADH-GOGAT* transcripts.

The analysis of the 5′ upstream region of the *NADH-GOGAT* gene led to the identification of four possible regulatory regions, one responsible for directing expression in the N_2-fixing zone, two positive elements, and one negative element. Earlier we reported that the 5′ upstream region of the *NADH-GOGAT* gene directs expression of the GUS reporter gene in the alfalfa root nodule meristem (zone I), invasion (zone II), interzone (zone II–III [*]), and N_2-fixing (zone III) zones (Vance et al., 1995). Detection of the NADH-GOGAT message by in situ hybridization showed that the transcript is absent in the meristem (zone I) and invasion (zone II) zones of the nodule. This discrepancy could be the result of two factors: (a) the integration site of the promoter reporter gene construct into the plant genome influences transcription and thus distorts localization; or (b) the GUS protein and/or reaction substrate could diffuse during the infiltration and incubation procedure and therefore be another source of distortion.

However, for constructs GLate and G1, plants with GUS enzyme activity closest to the mean had a histochemical staining pattern similar to the results obtained from in situ hybridization. These data indicate that the two constructs contain elements necessary for expression of the *NADH-GOGAT* gene in the N_2-fixing zone of a root nodule. By contrast, a consistent loss of N_2-fixing-zone specificity was observed in nodules of G2 plants, suggesting that an element for nodule-infected, cell-specific expression lies between G1 (−1064) and G2 (−655). It is interesting that this region contains an 88-bp direct repeat (Fig. 7E). Of the 408 bp found in the region controlling N_2-fixing-zone specificity, 176 bp or 43% of the sequence occur in this direct repeat. However, the conserved elements 5′-AAAGAT and 5′-CTCTT, which have been associated with nodule specificity of late-nodulin genes (Sandal et al., 1987; de Bruijn and Schell 1993), were found neither in the 88-bp direct repeat nor in the G1 (−1064) to G2 (−655) region. By comparing the 88-bp direct repeat against 5′ upstream regions of other nodulin and nodule-enhanced genes, we found a 14-bp AT-rich sequence also found in the alfalfa leghemoglobin promoter (5′-TTAATTAATAAATA-3′). This region contains a sequence similar to the proposed octanucleotide motif on the opposite strand (5′-AATAAATA-3′), which has been associated with positive regulatory elements in several other late-nodulin gene promoters (Forde et al., 1990). Using gel-mobility-shift analysis, it was demonstrated that this motif is part of the NAT2 binding site in the soybean leghemoglobin (*lbc3*) (Jensen et al., 1988) and the soybean *N23* promoter (Jacobsen et al., 1990). In French bean, the promoter of the nodule-enhanced GS (glnγ) contains this motif within two 21-bp AT-rich repeats that are binding sites for PNF-1 (*Phaseolus* nodule factor-1) (Forde et al., 1990). When the region of the glnγ promoter that contains these repeats was inserted in the −90 position of the cauliflower mosaic virus 35S promoter, the construct was able to direct expression of the GUS-reporter gene in birdsfoot trefoil root nodules (Shen et al., 1992). However, the function of AT-rich elements, which serve as binding sites for nuclear proteins, is still unclear. Although such elements are often closely associated with positive regulatory elements in a wide variety of plant genes (Forde, 1994), it has also been found that these AT-rich binding sites can be deleted without affecting gene expression (Forde, 1994).

Although the region between G1 (−1064) and G2 (−655) seems to be important for reporter-gene expression in the N_2-fixing zone of a root nodule, other than the AT-rich binding site, the deleted region does not contain regions with sequence homology to other reported sequences that have been associated with nodule specificity of late-nodulin genes (Sandal et al., 1987; Forde et al., 1990; de Bruijn and Schell 1993). These observations led us to two conclusions: (a) the deleted region may contain unknown elements responsible for nodule-specific expression; and (b) the deleted region contains elements involved in a physiological response of the plant cell, e.g. low oxygen partial pressure. Further analysis of this important region of the *NADH-GOGAT* promoter using finer deletions and gel-mobility-shift analysis may resolve this question.

Although construct G5 (−240) has the same histochemical staining as construct G4 (−343), we measured a signif-

icant decrease in GUS activity ($P < 0.01$), suggesting the presence of positive element(s) associated with the deleted region. A significant increase in enzyme activity ($P < 0.01$) was measured between deletion G5 (−240) and G6 (−151), suggesting the presence of negative element(s) associated with this region. However, sequence analysis of the deleted regions did not reveal similarities to previously reported positive and negative elements. Between deletion G6 (−151) and G7 (−82) we measured a significant decrease in GUS activity ($P < 0.01$) to background levels, indicating the presence of positive element(s) associated with this region. Although deletion G7 (−82) still contained the putative TATA box (−21), the region between G6 (−151) and G7 (−82) lies within the area generally associated with elements responsible for regulating the frequency of transcription initiation (Kuhlemeier et al., 1987). Such elements have been identified in animals as the conserved CAAT and GC boxes. However, in plants such boxes are often substituted (Kreis et al., 1986; Kuhlemeier et al., 1987) or absent (Kuhlemeier et al., 1987).

In this study we have extended the understanding of *NADH-GOGAT* in N_2 fixation and N assimilation by showing that the enzyme is encoded by a single gene and that *NADH-GOGAT* transcripts predominantly accumulate in the infected cell of the N_2-fixing zone, but do not require active N_2 fixation for initial expression. In addition, we have delimited several segments in the 5′ upstream region of *NADH-GOGAT* that affect reporter-gene expression. One of them between G1 (−1064) and G2 (−655) contains an 88-bp repeat that may affect expression in the N_2-fixing zone. Although these findings strengthen our original hypothesis that NADH-GOGAT represents a rate-limiting step in the assimilation of symbiotically fixed N in alfalfa nodules, further studies using antisense approaches are required to verify the strategic role of this important enzyme.

ACKNOWLEDGMENTS

We thank Ann Hirsch and Turlough Finan for generously sharing ineffective *S. meliloti* strains, Ann Hirsch and Mike Sadowsky for sharing the leghemoglobin cDNA and the *nifH* gene, and Gyorgy B. Kiss and Allen Smith for critically reading the manuscript. We give special thanks to Nikolaus Amrhein for his insightful remarks.

Received September 14, 1998; accepted December 9, 1998.

LITERATURE CITED

Anderson MP, Vance CP, Heichel GH, Miller SS (1989) Purification and characterization of NADH-glutamate synthase from alfalfa root nodules. Plant Physiol **90:** 351–358

Austin S, Bingham ET, Mathews DE, Shahan MN, Will J, Burgess RR (1995) Production and field performance of transgenic alfalfa (*Medicago sativa* L.) expressing *alpha*-amylase and manganese-dependent lignin peroxidase. Euphytica **85:** 381–383

Avila C, Marquez AJ, Pajuelo P, Cannell ME, Wallsgrove RM, Forde BG (1993) Cloning and sequence analysis of a cDNA for barley ferredoxin-dependent glutamate synthase and molecular analysis of photorespiratory mutants deficient in the enzyme. Planta **189:** 475–483

Baron AC, Tobin TH, Wallsgrove RM, Tobin AK (1994) A metabolic control analysis of the glutamine synthetase/glutamate synthase cycle in isolated barley (*Hordeum vulgare* L.) chloroplasts. Plant Physiol **105:** 415–424

Becker TW, Perrot-Rechenmann C, Suzuki A, Hirel B (1993) Subcellular and immunocytochemical localization of the enzymes involved in ammonia assimilation in mesophyll and bundle-sheath cells of maize leaves. Planta **191:** 129–136

Bingham ET (1991) Registration of alfalfa hybrid RegenSY germplasm for tissue culture and transformation research. Crop Sci **31:** 1098

Boland MJ, Benny AG (1977) Enzymes of nitrogen metabolism in legume nodules: purification and properties of NADH-dependent glutamate synthase from lupin nodules. Eur J Biochem **79:** 355–362

Chen F-L, Cullimore JV (1988) Two isoenzymes of NADH-dependent glutamate synthase in root nodules of *Phaseolus vulgaris* L. Plant Physiol **88:** 1411–1417

Chen F-L, Cullimore JV (1989) Location of two isoenzymes of NADH-dependent glutamate synthase in root nodules of *Phaseolus vulgaris* L. Planta **179:** 441–447

Cox KH, Goldberg RB (1988) Analysis of plant gene expression. *In* CH Shaw, ed, Plant Molecular Biology: A Practical Approach. IRL Press, Oxford, UK, pp 1–34

de Billy F, Barker DG, Gallusci P, Truchet G (1991) Leghemoglobin gene transcription is triggered in a single cell layer in the indeterminate nitrogen-fixing root nodule of alfalfa. Plant J **1:** 27–35

de Bruijn FJ, Schell J (1993) Regulation of plant genes specifically induced in developing and mature nitrogen-fixing nodules: *cis*-acting elements and *trans*-acting factors. *In* DPS Verma, ed, Control of Plant Gene Expression. CRC Press, Boca Raton, FL, pp 241–258

Egli MA, Griffith SM, Miller SS, Anderson MA, Vance CP (1989) Nitrogen assimilatory enzymes and enzyme protein during development and senescence of effective and plant gene-controlled ineffective alfalfa nodules. Plant Physiol **91:** 898–904

Fleming AJ, Mandel T, Roth I, Kuhlemeier C (1993) The patterns of gene expression in the tomato apical meristem. Plant Cell **5:** 297–309

Forde BG (1994) AT-rich elements (ATREs) in the promoter regions of nodulin and other higher plant genes: a novel class of *cis*-acting regulatory element? *In* L Nover, ed, Plant Promoters and Transcription Factors. Springer-Verlag, Heidelberg, Germany, pp 87–101

Forde BG, Freeman J, Oliver JE, Pineda M (1990) Nuclear factors interact with conserved A/T-rich elements upstream of nodule-enhanced glutamine synthetase from French bean. Plant Cell **2:** 925–939

Franssen HJ, Vijn I, Yang WC, Bisseling T (1992) Developmental aspects of the *Rhizobium*-legume symbiosis. Plant Mol Biol **19:** 89–107

Gantt SJ, Larson RJ, Farnham MW, Pathirana SM, Miller SS, Vance CP (1992) Aspartate aminotransferase in effective and ineffective alfalfa nodules. Cloning of a cDNA and determination of enzyme activity, protein, and mRNA levels. Plant Physiol **98:** 868–878

Goto S, Akagawa T, Kojima S, Hayakawa T, Yamaya T (1998) Organization and structure of NADH-dependent glutamate synthase gene from rice. Biochim Biophys Acta **1387:** 298–308

Gregerson RG, Miller SS, Petrowski M, Gantt JS, Vance CP (1993a) Molecular analysis of allelic polymorphism at the AAT2 locus of alfalfa. Mol Gen Genet **241:** 124–128

Gregerson RG, Miller SS, Twary SN, Gantt JS, Vance CP (1993b) Molecular characterization of NADH-dependent glutamate synthase from alfalfa nodules. Plant Cell **5:** 215–226

Groat GR, Vance CP (1981) Root and nodule enzymes of ammonia assimilation in alfalfa (*Medicago sativa* L.). Plant Physiol **67:** 1198–1205

Hayakawa T, Yamaya T, Kamachi K, Ojima K (1992) Purification, characterization, and immunological properties of NADH-dependent glutamate synthase from rice cell cultures. Plant Physiol **98:** 1317–1322

Heintzen C, Melzer S, Fischer R, Kappeler S, Apel K, Staiger D (1994) A light- and temperature-entrained circadian clock controls expression of transcripts encoding nuclear proteins with

homology to RNA-binding proteins in meristematic tissue. Plant J **5:** 799–813

Hirasawa M, Tamura G (1984) Flavin and iron-sulphur containing ferredoxin-linked glutamate synthase from spinach leaves. J Biochem **95:** 983–994

Jacobsen K, Lauren NB, Jensen EO, Marcker A, Poulsen C, Marcker KA (1990) HMG I-like proteins from leaf and nodule nuclei interact with different AT motifs in soybean nodulin promoters. Plant Cell **2:** 85–95

Jefferson RA (1987) Assaying chimeric genes in plants: the GUS gene fusion system. Plant Mol Biol Rep **5:** 387–405

Jensen EO, Marcker KA, Schell J, de Bruijn FJ (1988) Interaction of a nodule specific, *trans*-acting factor with distinct DNA elements in the soybean leghemoglobin *lbc3* 5′ upstream region. EMBO J **7:** 1265–1271

Kendall AC, Wallsgrove RM, Hall NP, Turner JC, Lea PJ (1986) Carbon and nitrogen assimilation in barley mutants lacking ferredoxin-dependent glutamate synthase. Planta **168:** 316–323

Knauff DB, Hirasawa M, Ameyibor E, Fu W, Johnson MK (1991) Spectroscopic evidence for a [3Fe-4S] cluster in spinach glutamate synthase. J Biol Chem **266:** 15080–15084

Kreis M, Williamson MS, Forde J, Schmutz D, Clark J, Buxton B, Pywell J, Marris C, Henderson J, Harris N, and others (1986) Differential gene expression in the developing barley endosperm. Philos Trans R Soc Lond B Biol Sci **314:** 355–366

Kuhlemeier C, Green PJ, Chua N-H (1987) Regulation of gene expression in higher plants. Annu Rev Plant Physiol Plant Mol Biol **38:** 221–257

Lam H-M, Coschigano KT, Oliveira IC, Melo-Oliveira R, Coruzzi GM (1996) The molecular-genetics of nitrogen assimilation into amino acid in higher plants. Annu Rev Plant Physiol Plant Mol Biol **47:** 569–593

Lea PJ, Robinson SA, Stewart GR (1990) The enzymology and metabolism of glutamine, glutamate and asparagine. *In* BJ Miflin, PJ Lea, eds, Biochemistry of Plants: Intermediary Nitrogen Metabolism, Vol 16. Academic Press, San Diego, CA, pp 121–159

Leigh VA, Reed JW, Hanks JF, Hirsch AM, Walker GC (1987) *Rhizobium meliloti* mutants that fail to succinylate their calcofluor-binding exopolysaccharide are defective in nodule invasion. Cell **70:** 579–587

Minchin FR, Witty JF, Sheely JF, Mueller M (1983) A major error in the acetylene reduction assay: decreases in nodular nitrogenase activity under assay conditions. J Exp Bot **34:** 641–649

Nalbantoglu B, Hirasowa M, Moomav C, Nguyen H, Knaff DB, Allen R (1994) Cloning and sequencing of the gene encoding spinach ferredoxin-dependent glutamate synthase. Biochim Biophys Acta **1183:** 557–561

Oliver G, Gosset G, Sanchez-Pescador R, Lozoya E, Ku LM, Flores N, Becerril B, Valle F, Bolivar F (1987) Determination of the nucleotide sequence for the glutamate synthase structural genes in *Escherichia coli* K12. Gene **60:** 1–11

Pathirana MS, Samac DA, Roeven R, Yoshioka H, Vance CP, Gantt JS (1997) Analyses of phosphoenolpyruvate carboxylase gene structure and expression in alfalfa nodules. Plant J **12:** 293–304

Peterson MA, Barnes DK (1981) Inheritance of ineffective nodulation and non-nodulation traits in alfalfa. Crop Sci **21:** 611–616

Pladys D, Vance CP (1993) Proteolysis during development and senescence of effective and plant gene-controlled ineffective alfalfa nodules. Plant Physiol **103:** 379–384

Sakakibara H, Kawabata S, Hase T, Sugiyama T (1992) Differential effects of nitrate and light on the expression of glutamine synthetases and ferredoxin-dependent glutamate synthase in maize. Plant Cell Physiol **33:** 1193–1198

Sakakibara H, Watanabe M, Hase T, Sugiyama T (1991) Molecular cloning and characterization of complementary DNA encoding for ferredoxin-dependent glutamate synthase in maize leaf. J Biol Chem **266:** 2028–2035

Sambrook J, Fritsch EF, Maniatis T (1989) Molecular Cloning: A Laboratory Manual. Cold Spring Harbor Laboratory Press, Cold Spring Harbor, NY

Sandal NN, Bojsen K, Marcker KA (1987) A family of nodule specific genes from soybean. Nucleic Acids Res **15:** 1507–1519

Scheres B, van Engelen F, van der Knaap E, van der Wiel C, van Kammen A, Bisseling T (1990) Sequential induction of nodulin gene expression in the developing pea nodule. Plant Cell **2:** 687–700

Shen W-J, Williamson MS, Forde BG (1992) Functional analysis of the promoter region of a nodule-enhanced glutamine synthetase gene from *Phaseolus vulgaris* L. Plant Mol Biol **19:** 837-846

Sommerville CR, Ogren WL (1980) Inhibition of photosynthesis in *Arabidopsis* mutants lacking in leaf glutamate synthase activity. Nature **286:** 257–259

Temple SJ, Heard J, Ganter G, Dunn K, Sengupta-Gopalan C (1995) Characterization of a nodule-enhanced glutamine synthetase from alfalfa: nucleotide sequence, *in situ* localization, and transcript analysis. Mol Plant Microbe Interact **8:** 218–227

Temple SJ, Vance CP, Gantt JS (1998) Glutamate synthase and nitrogen fixation. Trends Plant Sci **3:** 51–56

Vance CP, Gantt JS (1992) Control of nitrogen and carbon metabolism in root nodules. Physiol Plant **85:** 266–274

Vance CP, Gregerson RG, Robinson DL, Miller SS, Gantt JS (1994) Primary assimilation of nitrogen in alfalfa nodules: molecular features of the enzymes involved. Plant Sci **101:** 51–64

Vance CP, Miller SS, Gregerson RG, Samac DA, Robinson DL, Gantt JS (1995) Alfalfa NADH-dependent glutamate synthase: structure of the gene and importance in symbiotic N_2 fixation. Plant J **8:** 345–358

Vasse J, de Billy F, Camut S, Truchet G (1990) Correlation between ultrastructure differentiation of bacteroids and nitrogen fixation. J Bacteriol **172:** 4295–4306

Vijn I, Yang W-C, Pallisgard N, Jensen EO, van Kammen A, Bisseling T (1995) VsENOD5, VsENOD12, and VsENOD40 expression during *Rhizobium*-induced nodule formation in *Vicia sativa* roots. Plant Mol Biol **28:** 1111–1119

Wallsgrove RM, Lea PJ, Miflin BJ (1979) Distribution of the enzymes of nitrogen assimilation within the pea leaf cell. Plant Physiol **63:** 232–236

Yarosh OK, Charles TC, Finan TM (1989) Analysis of C4-dicarboxylate transport genes in *Rhizobium meliloti*. Mol Microbiol **3:** 813–824

Zehnacker C, Becker TW, Suzuki A, Carrayol E, Caboche M, Hirel B (1992) Purification and properties of tobacco ferredoxin-dependent glutamate synthase, and isolation of corresponding cDNA clones: light-inducibility and organ-specificity of gene transcription and protein expression. Planta **187:** 266–274